Rotational magnetic losses in non-oriented Fe-Si and Fe-Co laminations up to the kHz range

C Appino, Olivier de La Barrière, C Beatrice, F Fiorillo, C Ragusa

Rotational magnetic losses in non-oriented Fe-Si and Fe-Co laminations up to the kHz range

C. Appino[1a], O. de la Barrière[2], C. Beatrice[1], F. Fiorillo[1], and C. Ragusa[3]

[1]Istituto Nazionale di Ricerca Metrologica (INRIM), Electromagnetics Department, Strada delle Cacce 91, 10135 Torino, Italy
[2]SATIE, CNRS, UniverSud, 61 av. du Président Wilson, F-94230 Cachan, France
[3]Politecnico di Torino, Dipart. Energia, C.so Duca degli Abruzzi 24, 10129 Torino, Italy

Literature data on the energy loss behavior of steel sheets under rotating induction are restricted to quite low frequencies, i.e. up to a few hundreds of hertz. This is not sufficient to predict the loss in high-speed electrical machines, where frequencies in the kilohertz range are commonly encountered. We have overcome this difficulty by making loss measurements under alternating and circular induction in 0.2 mm thick Fe-(3 wt%)Si and $Fe_{49}Co_{49}V_2$ sheets using a specially designed experimental setup. Peak polarization levels and frequencies up to 1.6 T at 2 kHz have been reached in the Fe-Si laminations, whereas the Fe-Co alloy, endowed with much higher permeability, has been characterized up to 2.1 T at 5 kHz. In the first part of this paper, the measured loss behavior versus peak polarization and magnetizing frequency is presented. In the second part, a loss model for circular induction is proposed, taking into account the skin effect. To this end, we have derived a simple magnetic constitutive law for the material, assumed to be isotropic, and we have introduced it into the electromagnetic diffusion equation. The solution of this equation by an iterative algorithm provides the induction profile across the sample thickness and eventually the classical loss component, which represents the major contribution to the total loss at high frequencies. Good agreement with the experiments is obtained.

***Index Terms*—Magnetic losses, circular induction, non-oriented magnetic steel, skin effect.**

I. Introduction

HIGH SPEED electrical machines are very promising in terms of torque density [1], and therefore they are potentially interesting for embedded applications, such as on-board aircraft electrical plant [2]. A correct prediction of the energy efficiency at the design stage requires an accurate characterization of the material in the frequency range encountered in such machines (i.e. up to a few kilohertz). Thus, a physically based model must be derived from these data, in order to predict the loss for the various induction wave shapes encountered in electrical machines [2]. Modeling can be challenging, because of the skin effect, a phenomenon that cannot be neglected in the kilohertz range [2][3].

The experimental approach to medium frequency measurements under alternating field in soft magnetic laminations is well assessed and a specific standard up to 10 kHz exists [4]. Loss prediction taking into account the skin effect has also been successfully dealt with in the framework of the loss separation concept by solving the diffusion equation under an hysteretic magnetic constitutive law [2][3].

Two-dimensional (2D) induction loci are ubiquitous in electrical machines [5], but for these conditions no measurement standards have been developed and the theoretical approach is equally limited, with no consideration for the skin effect [6] [7]. Most laboratories use cross-shaped apparatus to generate a circular induction in the center of a square sheet [8], although this may result in poor homogeneity of the induction across the sample.

To overcome the problem of field inhomogeneity, an experimental setup based on a three-phase magnetizer and a circular sample, operating up to 200 Hz has been developed [7]. Its upper frequency has been recently extended to the kilohertz range for 2D testing [9], whereas 3D investigation of Soft Magnetic Composites (SMC) at such frequencies has been recently proposed by Li *et al.* [10].

In this paper we discuss rotational loss results obtained up to 5 kHz in 0.2 mm thick Fe-(3wt%)Si and $Fe_{49}Co_{49}V_2$ laminations by means of a three-phase magnetizer. After presenting significant examples of broadband alternating and rotational loss measurements, obtained on a wide range of peak induction values, we consider the problem of loss prediction taking into account the skin effect, a matter never addressed so far for rotational magnetization. A simplified non-linear magnetic constitutive law under rotating field is thus worked out and introduced into the electromagnetic diffusion equation, in order to describe the classical loss, the largest dissipative contribution at high frequencies. Loss separation is thereby achieved. The relationship between the classical loss formulations with and without the skin effect can in this way be considered and quantified.

II. Experimental procedure and results

Hysteresis loops and energy losses have been measured under alternating and rotational flux on standard Epstein strips and 80 mm diameter disk-shaped samples, cut out of commercial non-oriented Fe-(3wt%)Si sheets (conductivity $\sigma = 1.92\times10^6$ S/m, density $\delta = 7650$ kg/m^3, thickness $d = 0.194$ mm, saturation polarization $J_s = 2.01$ T) and $Fe_{49}Co_{49}V_2$ ($\sigma = 2.27\times10^6$ S/m, $\delta = 8120$ kg/m^3, $d = 0.201$ mm, $J_s = 2.35$ T). The Fe-Si and Fe-Co samples have been characterized between 0.1 T – 1.6 T and 0.1 T – 2.1 T, respectively. Alternating field experiments have been performed under controlled sinusoidal waveform on both materials, using a standard Epstein frame (IEC 60404-10), in the range 2 Hz - 10 kHz. A setup exploiting the so-called fieldmetric method,

[a] Corresponding author, e-mail : c.appino@inrim.it

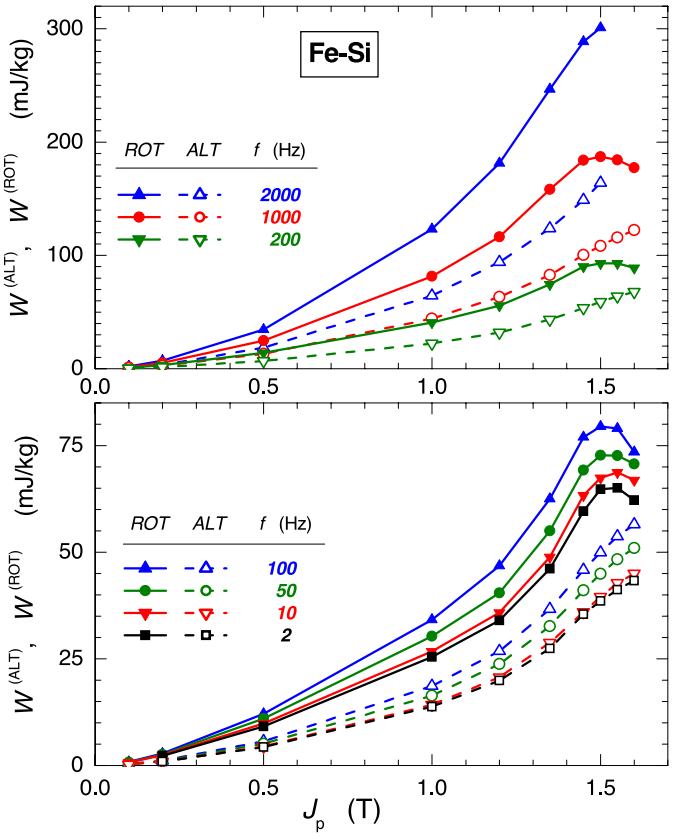

Fig. 1. Fe-Si alloy. Behavior of the measured alternating and rotational losses versus peak polarization J_p at selected frequencies.

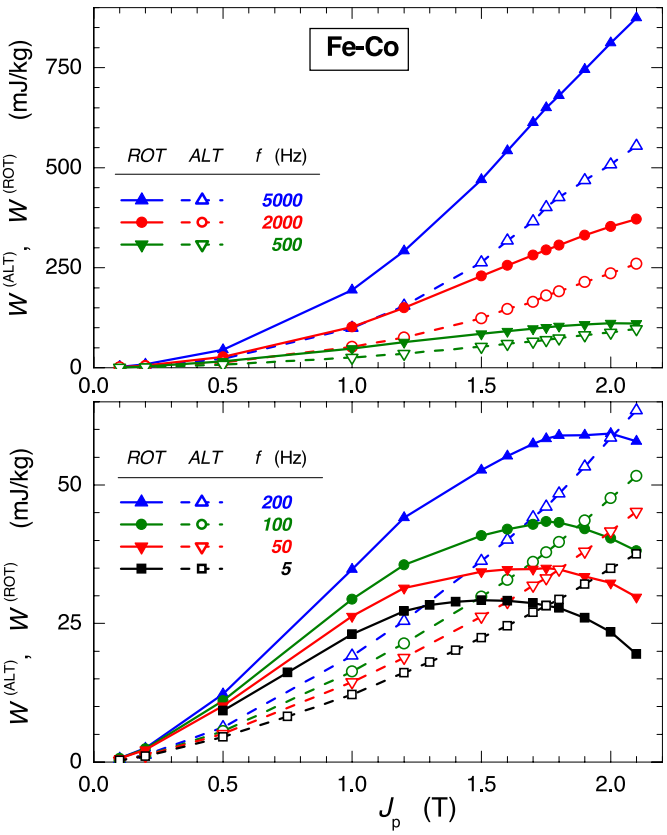

Fig. 2. Fe-Co alloy. Same as Fig. 1.

described in [9] and used in [11], has been instead employed for measurements under circular polarization on disk samples, with the frequency f extending from 2 Hz to 2 kHz and from 5 Hz to 5kHz in the Fe-Si and Fe-Co sheets, respectively. The loss values are obtained by averaging the measurements performed under clockwise and counterclockwise rotation. The circular flux loci are achieved via a digital feedback algorithm implementing the principle of contraction mapping [12]. The behavior of alternating $W^{(ALT)}$ and rotational $W^{(ROT)}$ energy losses versus the peak polarization J_p is illustrated in Fig. 1 (Fe-Si alloy) and Fig. 2 (Fe-Co alloy), at selected frequencies. It is noted that in the present experiments J_p coincides to all practical extent with the peak induction B_p.

The behavior of losses versus f and J_p (i.e. B_p) is investigated exploiting the principle of separation of losses: $W = W_{hyst} + W_{class} + W_{exc}$, being W_{hyst}, W_{class}, and W_{exc} the hysteresis, classical and excess components, respectively. W_{hyst} is obtained after extrapolation to $f = 0$ of the experimental total loss W versus f curve, according to the Statistical Theory of Losses [11]. In the absence of skin effect, the classical loss per unit volume is given, for sinusoidal induction, by the equation

$$W_{class}^{(ALT)}(B_p, f) = \frac{p^2}{6} s d^2 B_p^2 f \qquad [J/m^3] \qquad (1)$$

[13] and under rotational flux it is $W_{class}^{(ROT)} = 2\, W_{class}^{(ALT)}$. In addition, the excess loss component is, both under alternating and rotational induction, $W_{exc}(f) \propto f^{1/2}$ [14]. The analysis of these results shows, however, that skin effect interferes strongly with the material response, especially in the high-permeability Fe-Co laminations, and must be duly considered.

III. Rotational Losses: The Role of the Skin Effect

A method for the assessing the loss behavior under high frequency rotating induction is now discussed. To this end, simplifying assumptions are invoked, in order to work out a constitutive law for the material under circular polarization.

The material is assimilated to an equivalent isotropic medium, so that we can resort to the concept of complex permeability. The ensuing non-linear diffusion equation is then numerically solved by an iterative algorithm. Simulations applied on the Fe-Co samples, exhibiting important skin effect and dominant classical loss contribution in the kHz range, are shown to be in good agreement with the experiments.

A. Derivation of a simplified magnetic constitutive law

Given a circular induction vector $\boldsymbol{B}$, the constitutive equation $\boldsymbol{B}(\boldsymbol{H}_0)$, where $\boldsymbol{H}_0$ is the corresponding rotating magnetic field, is obtained as follows:

- A rate independent relationship is assumed, i.e. only static hysteresis is taken into account (as done in [3] for alternating field) to derive $\boldsymbol{B}(\boldsymbol{H}_0)$.
- The material anisotropy, pretty small in the investigated materials, is neglected. Accordingly, given a circular induction vector $\boldsymbol{B}$, we define a corresponding circular magnetic field $\boldsymbol{H}_0$ of constant modulus, leading $\boldsymbol{B}$ by a constant phase shift [15].
- For each circular experimental $B_p = |\boldsymbol{B}|$ value and each frequency f, the magnetic field locus is measured, and a circle having the same area is considered. The radius of such a circle gives the amplitude of the circular magnetic field $H(f) = |\boldsymbol{H}(f)|$ in the equivalent isotropic material. This quantity,

obtained versus f for each induction value, once extrapolated to $f = 0$, provides the limiting value $H_0 = |\boldsymbol{H}_0|$ and the associated modulus $\mu \equiv \mu(H_0) = B_p/H_0$ of the complex permeability (see Fig. 3).

– The spatial phase shift θ_{hyst} between $\boldsymbol{B}$ and $\boldsymbol{H}_0$ (Fig. 3), corresponding to the rotational hysteresis loss ($f \to 0$) $W_{hyst}^{(ROT)}(B_p)$, is then obtained as

$$q_{hyst} \circ q_{hyst}(H_0) = \arcsin\left[\frac{W_{hyst}^{(ROT)}(B_p)}{2\pi H_0 B_p}\right] \qquad (2)$$

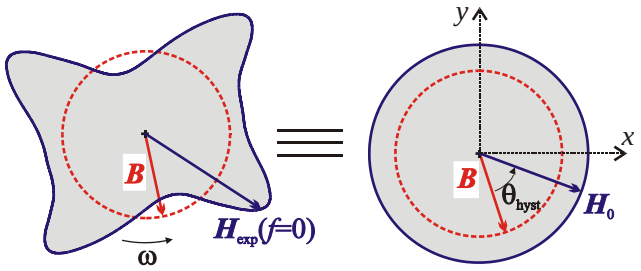

Fig. 3. Derivation of the equivalent isotropic material properties. The gray regions have same area.

The experimental quantities $\mu(H_0)$ and $\theta_{hyst}(H_0)$ are given in Fig. 4 for the investigated Fe-Co sheets.

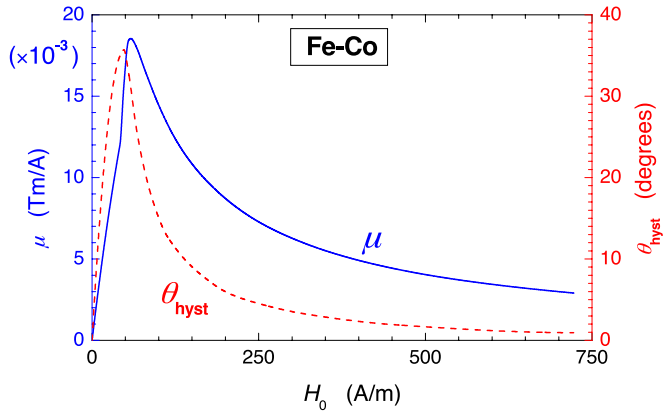

Fig. 4. Fe-Co sheets. Modulus $\mu(H_0)$ and spatial phase shift $\theta_{hyst}(H_0)$ of the complex permeability $\underline{\mu}$.

In a Cartesian reference frame xyz, with the xy plane corresponding to the lamination mid-plane and the origin of the z-axis taken in the center of the lamination, $\boldsymbol{H}_0$ and $\boldsymbol{B}$ are phase-shifted vectors rotating in the xy plane and their projection along a fixed direction (e.g. the x axis) is a sinusoidal function. The constitutive equation along such direction is

$$\underline{B}_x = \underline{\mu}\left(|\underline{H}_x|\right)\underline{H}_x, \qquad (3)$$

where $\underline{\mu}$ is the complex permeability

$$\underline{\mu}(H_0) = \mu(H_0)\exp\left[-i\theta_{hyst}(H_0)\right]. \qquad (4)$$

Under rotational regime, B_p, H_0 and the modulus and spatial phase shift of $\underline{\mu}$ are constant over the period. This situation basically differs from the one occurring under alternating fields, where the constitutive relationship identifies with the hysteresis loop and consequently calls for an hysteresis model (e.g. the Preisach model [3]).

B. *Diffusion equation*

The diffusion equation of magnetic field under rotational regime is now worked out assuming an infinitely extended sheet plane xy, so that all the local quantities depend only on z. We obtain in complex notation, e.g. along the x-axis, the following equation:

$$\frac{\partial^2 \underline{H}_x(z)}{\partial z^2} = i\omega s \underline{B}_x(z), \qquad (5)$$

being $i^2 = -1$ and $\omega = 2\pi f$. Given the symmetry of the problem, an identical equation is written for the y-coordinate and only the $0 < z < d/2$ portion along the sheet thickness needs to be considered. The constitutive law (3) now becomes a link between $B_x(z)$ and $H_x(z)$. We accordingly obtain:

$$\begin{cases} \dfrac{\partial^2 \underline{H}_x(z)}{\partial z^2} = i\omega s \underline{\mu}\left(|\underline{H}_x(z)|\right)\underline{H}_x(z) \\ \dfrac{\partial \underline{H}_x(z)}{\partial z}\bigg|_{z=0} = 0 \quad \text{and} \quad \dfrac{\partial \underline{H}_x(z)}{\partial z}\bigg|_{z=d/2} = i\omega s \dfrac{d}{2} B_p \end{cases}. \qquad (6)$$

The first boundary condition is derived from the symmetry of the magnetic field profile with respect to the $z = 0$ plane, whereas the second one imposes that the mean induction across the lamination cross-section is B_p. The non-linear system (6) can be solved through a finite element method coupled with the Fixed Point (FP) technique [3]. The total loss is calculated via the Poynting theorem, whereas the classical component is obtained after volume integration of the squared current density. An example of so-calculated rotational loss is given in Fig. 5, where the energy loss measured at $f = 5$ kHz versus J_p is compared with the computed total loss $W^{(ROT,\,FP)}$, the sum of the measured hysteresis loss and the calculated classical component $W_{class}^{(ROT,\,FP)}$. At such a frequency, where the skin effect is fully developed, W_{class} overwhelmingly dominates (more than 95 % of the total loss) and the prediction neglecting the excess loss component, is accurate.

C. *Classical loss analysis*

Having devised a full treatment of the classical rotational losses, we can verify to what extent a model neglecting the skin effect can approximate the experimental results. To this end we consider the ratio F_{class} between the classical losses calculated with and without the skin effect.

If the classical loss is computed from eq. (6) we are dealing with the $F_{class}^{(FP)}$ ratio. In this case the non-linear behavior of the material is accounted for by the dependence of $\underline{\mu}$ on the depth z.

A simplified model might also be proposed, as in [16], and an analytical expression of F_{class} as a function of the ratio d/δ (being $\delta = 1/(\pi\mu\sigma f)^{1/2}$ the standard skin depth) could be derived under alternating field assuming constant real permeability μ depending on the peak induction B_p only. When dealing with circular induction, which implies a (complex) permeability $\underline{\mu}$ constant over the period, a same

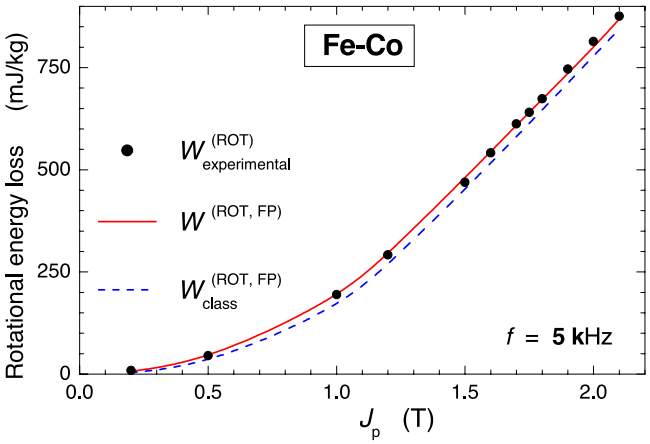

Fig. 5. Fe-Co alloy. Experimental and predicted loss figures vs. J_p at f = 5 kHz. The negligible role of the excess and hysteresis loss components is apparent at high J_p values.

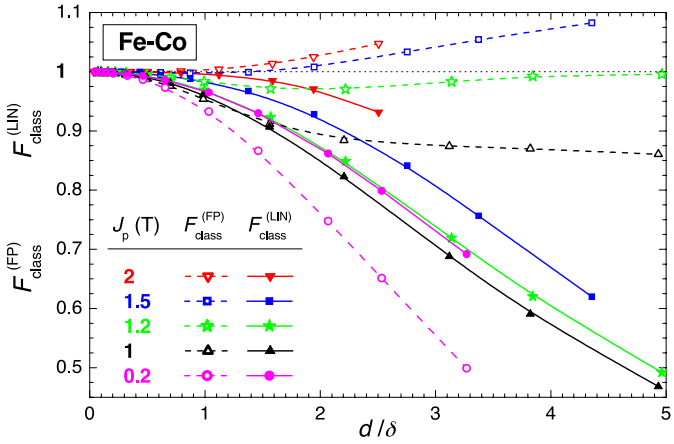

Fig. 6. Ratios F_{class} between the classical losses computed with and without accounting for the skin effect. $F_{class}^{(FP)}$ and $F_{class}^{(LIN)}$ represent the ratios obtained via the Fixed Point and the linear methods, respectively. d is the sheet thickness and δ the standard skin depth.

approach could be adopted, assuming $\underline{\mu}$ constant across the sheet depth, depending again on B_p, according to the constitutive relations (3) and (4) (see also Fig. 4). This procedure leads to a linear equation that can be analytically solved. The ensuing ratio is accordingly denoted $F_{class}^{(LIN)}$.

The comparison between $F_{class}^{(FP)}$ and $F_{class}^{(LIN)}$ is shown in Fig. 6, for f ranging from DC to 5 kHz. Remarkably, the material non-linearity at high induction values implies $F_{class}^{(FP)} > 1$, a result that cannot be attained by $F_{class}^{(LIN)}$, which assumes $\underline{\mu}$ constant across the sheet depth. Thus, by neglecting the skin effect (i.e. assuming $F_{class} = 1$) in the computation of the classical losses at high inductions, we obtain better results than using a linear diffusion model, which tends to underestimate the loss.

IV. Conclusions

Energy loss results in 0.2 mm thick Fe-Si and Fe-Co laminations, excited with circular induction loci up to high frequencies have been discussed. The ranges 2 Hz - 2 kHz for the Fe-Si samples, and 5 Hz - 5 kHz for the Fe-Co ones have been, in particular, considered in experiment and theory, providing a broad experimental background for the use of these materials in high-speed machines.

The problem of the loss prediction has been addressed through a simplified magnetic constitutive law, which has been introduced in the electromagnetic diffusion equation, leading to good predictive results. Special attention has been devoted to the analysis of the classical loss component, which represents the dominant dissipative contribution at high frequencies. The limited predicting power of the linear skin effect models has therefore been brought to light.

V. Acknowledgments

The authors acknowledge support by the MIUR-PRIN Project MEA 2009LKCT3E "*Advanced characterization and modeling of magnetic materials for the More Electric Aircraft*", e-méca project of the Agence Nationale de la Recherche (France), and MIUR Progetto Premiale *"Misure e modelli per una gestione efficiente e sostenibile dell'energia elettrica"*.

VI. References

[1] S. Niu, S. Ho, W. Fu, and J. Zhu, "Eddy Current Reduction in High-Speed Machines and Eddy Current Loss Analysis With Multislice Time-Stepping Finite-Element Method," *IEEE Trans. Magn.*, vol. 48, pp. 1007-1010, 2012.

[2] O. Bottauscio, G. Serra, M. Zucca, and M. Chiampi, "Role of Magnetic Materials in a Novel Electrical Motogenerator for the More Electric Aircraft," *IEEE Trans. Magn.*, vol. 50, pp. 1-4, 2014.

[3] C. Beatrice *et al.*, "Broadband Magnetic Losses in Fe-Si and Fe-Co Laminations," *IEEE Trans. Magn.*, vol. 50, pp. 1-4, 2014.

[4] IEC Standard Publication 60404-10, Methods of measurement of magnetic properties of magnetic steel sheet and strip at medium frequencies, 1988, Geneva, IEC Central Office.

[5] O. Bottauscio, M. Chiampi, A. Manzin, and M. Zucca, "Additional Losses in Induction Machines under Synchronous No-Load Conditions," *IEEE Trans. Magn.*, vol. 40, pp. 3254-3261, 2004.

[6] C. Ragusa, C. Appino, and F. Fiorillo, "Comprehensive investigation of alternating and rotational losses in non-oriented steel sheets," *Przegląd Elektrotechniczny*, vol. 85, pp. 7-10, 2009.

[7] C. Appino, F. Fiorillo, and C. Ragusa, "One-dimensional/two-dimensional loss measurements up to high inductions," *J. Appl. Phys.*, vol. 105, no. 7, pp. 07E718-1-07E718-3, 2009.

[8] J.G. Zhu and V.S. Ramsden, "Two dimensional measurement of magnetic field and core loss using a square specimen tester," *IEEE Trans. Magn.*, vol. 29, pp. 2995-2997, 1993.

[9] O. de la Barriere *et al.*, "Extended frequency analysis of magnetic losses under rotating induction in soft magnetic composites," *J. Appl. Phys.*, vol. 111, no. 7, pp. 07E325-07E327, 2012.

[10] Y. Li *et al.*, "Study on Rotational Hysteresis and Core Loss Under Three-Dimensional Magnetization," *IEEE Trans. Magn.*, vol. 47, no. 10, pp. 3520-3523, 2011.

[11] O. de la Barrière, C. Appino, C. Ragusa, F. Fiorillo, F. Mazaleyrat and M. LoBue, "High-frequency rotational losses in different soft magnetic composites," *J. Appl. Phys.*, vol. 115, pp. 17A331- 17A333, 2014.

[12] C. Ragusa and F. Fiorillo, "A three-phase single sheet tester with digital control of flux loci based on the contraction mapping principle," *J. Magn. Magn. Mater.*, vol. 304, pp. e568-e570, 2006.

[13] G. Bertotti, *Hysteresis in Magnetism*, Academic Press, New York, (1998).

[14] C. Appino, C. Ragusa, F. Fiorillo, "Can rotational magnetization be theoretically assessed?", International Journal of Applied Electromagnetics and Mechanics, vol. 44, pp. 355-370, 2014.

[15] I.D. Mayergoyz, F.M. Abdel-Kader, F.P. Emad, "On penetration of electromagnetic fields into nonlinear conducting ferromagnetic media," *J. Appl. Phys.*, vol. 55, no. 3, pp. 618-628, 1984.

[16] G. Grandi, M.K. Kazimierczuk, A. Massarini, U. Reggiani, G. Sancineto, "Model of laminated iron-core inductors for high frequencies," *IEEE Trans. Magn.*, vol. 40, no. 4, pp. 1839-1845, 2004.